ORGANOMETALLICS

Article

pubs.acs.org/Organometallics

Bite Angle Effects of κ^2P-dppm vs κ^2P-dppe in Seven-Coordinate Complexes: A DFT Case Study

Aneesh Chacko, Ubong R. Idem, Chatin H. Bains, Lynn M. Mihichuk, and Allan L. L. East*

Department of Chemistry and Biochemistry, University of Regina, Regina, Saskatchewan S4S 0A2, Canada

Supporting Information

ABSTRACT: This paper predicts the effects of replacing dppm (bis(diphenylphosphino)methane) with dppe (1,2-bis(diphenylphosphino)ethane) in seven-coordinate organometallic complexes by employing density functional theory (DFT) computations for a case example: $WI_2(CO)(\kappa^2P$-dppm$)(\eta^2{:}\eta^2$-nbd) (nbd = norbornadiene), an intermediate in the W(II)-catalyzed ring-opening metathesis polymerization (ROMP) of nbd. Effects on both structure and ligand binding energy (i.e., reactivity) were investigated. For the known W−dppm complex (crystal structure provided here), of 37 energy-distinct stereoisomers found, only one low-energy stereoisomer is predicted, and it agrees with the known X-ray crystal structure, lending faith to the conformer search procedure. For the as yet unknown W−dppe complex, of 31 energy-distinct stereoisomers found, two low-energy stereoisomers are predicted. The computed DFT ligand binding energies {W−P, W−ene, W−CO, W^+-I^-} are {9, 17, 44, 102} kcal mol^{-1} for the W−dppm complex and {3, 15, 37, 95} for the W−dppe complex. The conclusion is that the increased PWP bite angle of dppe vs dppm will reduce *all* ligand binding energies due to increased interligand steric repulsion.

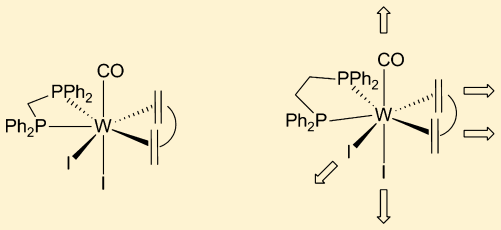

with dppm with dppe

1. INTRODUCTION

In homogeneous catalysis, ligands in the coordination sphere of the metal-centered organometallic catalyst can have a significant impact on reaction rate and product distribution, and the effects of the ligands can be either electronic or steric. An admirable example of the study of ligand effects is the work on hydroformylation of alkenes by van Leeuwen and co-workers:[1,2] they have carefully studied what is primarily[3,4] steric effects by using different series of bidentate diphosphino ligands with tunable PMP bite angles, monitoring changes in activity and regiospecificity. With ordinary nonbulky diphosphino ligands and Rh(I) catalysts, increasing the bite angle generally increased the reaction rate,[2a] but with very bulky ligands, increasing the bite angle over the same range generally *decreased* the reaction rate.[2b] van Leeuwen explained this as a change in the rate-limiting step,[2b] which we suspect follows a general steric rule: if the rate increases with increased bite angle, the rate-limiting step is likely one in which steric crowding decreases (e.g., decrease in coordination number), while if the rate decreases with increased bite angle, the rate-limiting step is likely one in which steric crowding increases (e.g., increase in coordination number).

The Rh(I) catalysts in the hydroformylation work above are five-coordinate. Such steric effects on bond activation by four-coordinate Pd complexes have been studied computationally by Bickelhaupt and co-workers,[5] with results in line with the second half of the rule. Our interest is in seven-coordinate W complexes, and in particular their ability to spontaneously initiate the ring-opening metathesis polymerization (ROMP) of norbornadiene (nbd) without the need of a preformed metal alkylidene.[6−11] Using the catalyst $WI_2(CO)_3(\kappa^2P$-dppm) (dppm = bis(diphenylphosphino)methane, $Ph_2PCH_2PPh_2$), an nbd-containing intermediate was isolated as the seven-coordinate complex $WI_2(CO)(\kappa^2P$-dppm$)(\eta^2{:}\eta^2$-nbd).[6] We are attempting to gain insight into how this complex proceeds toward the first reactive metal alkylidene in the polymerization cycle (Figure 1). In this vein, it was of interest to apply the above bite angle rule to seven-coordinate species, by trying to predict how substitution of dppm with dppe (1,2-bis(diphenylphosphino)ethane, $Ph_2PCH_2CH_2PPh_2$) would affect structure and/or reactivity.

Some hypotheses for the nbd activation stage have been explored via DFT computations by Szymańska-Buzar and co-workers[12,13] and extended by East and co-workers:[14,15] the latter predicted high activation barriers of over 45 kcal mol^{-1} for unimolecular rearrangement pathways[14] but found activation barriers half this size from an oxidative coupling of two nbd monomers.[15] Hence, assuming an oxidative coupling activation mechanism, the seven-coordinate intermediates would presumably undergo loss of ligand (7 to 6), addition of a second nbd (6 to 7), oxidative coupling (7 to 7), and finally a 1,4-H-shift (7 to 6). Given the uncertainty in the mechanism, the time-comsuming need for conformer searches, and the desire to be general to apply to other reactions, this paper is concerned only with effects on the 7-to-6 coordination-decreasing steps. Hence, the computational goals of this work were ligand binding energies for both $WI_2(CO)(\kappa^2P$-dppe$)(\eta^2{:}\eta^2$-nbd) and $WI_2(CO)(\kappa^2P$-dppm$)(\eta^2{:}\eta^2$-nbd).

Received: July 5, 2013
Published: September 18, 2013

   dx.doi.org/10.1021/om400667t | *Organometallics* 2013, 32, 5374−5383

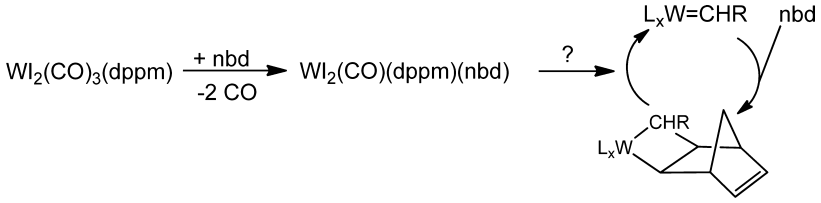

Figure 1. Assumed pathway for ROMP of nbd using the catalyst $WI_2(CO)_3(\kappa^2P\text{-dppm})$. In the polymerization cycle at the right, the R group gets progressively larger as each nbd is added. It is not yet known how the first intermediate proceeds to the polymerization cycle.

Large molecules have many stereoisomers which could span a large energy range; therefore, a proper computation of ligand binding energies requires serious effort in stereoisomer searches. Hence, such searches were performed for the ten compounds in Table 1: the proposed dppe-containing seven-coordinate parent **1**, the four compounds **2**–**5** that could immediately result from W–X dissociation, and similarly the previously isolated dppm-containing parent **6** and its six-coordinate fragmented compounds **7**–**10**.

Table 1. Molecules Studied in This Work

		molecule label	
category	formula	dppe case	dppm case
parent	$WI_2(CO)(\kappa^2P\text{-dppx})(\eta^2{:}\eta^2\text{-nbd})$	**1**	**6**
W–P scission	$WI_2(CO)(\kappa^1P\text{-dppx})(\eta^2{:}\eta^2\text{-nbd})$	**2**	**7**
W–π_{CC} scission	$WI_2(CO)(\kappa^2P\text{-dppx})(\eta^2\text{-nbd})$	**3**	**8**
W–CO scission	$WI_2(\kappa^2P\text{-dppx})(\eta^2{:}\eta^2\text{-nbd})$	**4**	**9**
W^+–I^- scission	$[WI(CO)(\kappa^2P\text{-dppx})(\eta^2{:}\eta^2\text{-nbd})]^+$	**5**	**10**

2. COMPUTATIONAL METHODOLOGY

All computations were performed using the Gaussian 03 (Rev. E.01) and Gaussian 09 (Rev. C.01) software packages.[16] The bulk of the calculations involved stereoisomer searches (full geometry optimizations) at the BP86/basis1 level of density functional theory to be consistent with earlier work.[14,15] The basis mixture "basis1" consists of the RDZP and ITZ2DF basis sets for the tungsten and iodide atoms, respectively,[14] the 6-31G(d) double-ζ basis set for the nbd ligand, carbonyl ligand, and the two phosphorus nuclei of the dppe and dppm ligands, and the single-ζ STO-3G basis set for all remaining atoms in dppe and dppm. The pseudo=read command was employed to include the LANL2DZ pseudopotential for core electrons on the I and W atoms.[17,18] The BP86/basis1 electronic energies of stereoisomers are presented as E_{rel}, i.e. relative to the energy of the lowest energy isomer (E_{lowest} = −2151.4844 and −2112.6415 au for the dppe and dppm complexes, respectively), and these "appearance energies" were used to estimate ligand binding energies at the BP86/basis1 level. Cartesian coordinates of all these optimized stereoisomers are available in the Supporting Information.

A variety of corrections were considered for improvement of the BP86/basis1 ligand binding energies. Zero-point vibrational energy corrections (ZPVE) were computed from BP86/basis1 frequency runs as half the sum of the unscaled harmonic frequencies. Solvation effects, ignoring nonelectrostatic effects as is Gaussian09's default, were computed with Gaussian09's polarizable continuum model[19] SCRF=(solvent=toluene), using BP86/basis1 single-point runs. Dispersion attraction effects (known to be lacking in DFT) were computed with single-point BP86/basis1 runs using IOp(3/124=3) in Gaussian 09 Revision C.01; this IOp added the 2006 DFT-D (now called "DFT-D2") basis-set-independent dispersion attraction correction of Grimme,[20] with the BP86-appropriate term scaling factor s_6 = 1.05, for every atom pair AB in the system. An improved-basis-set correction was computed with single-point BP86/basis2//BP86/basis1 runs, where basis2 is the same as basis1 except all STO-3G use was replaced with 6-31G(d) use; this increased the number of basis functions of **1** (the largest molecule here) from 419 to 677. Finally, some reoptimization of stereoisomer geometries was done with the BP86/basis2 level of theory, and a geometry relaxation effect due to improved basis was computed by subtracting these geometry-

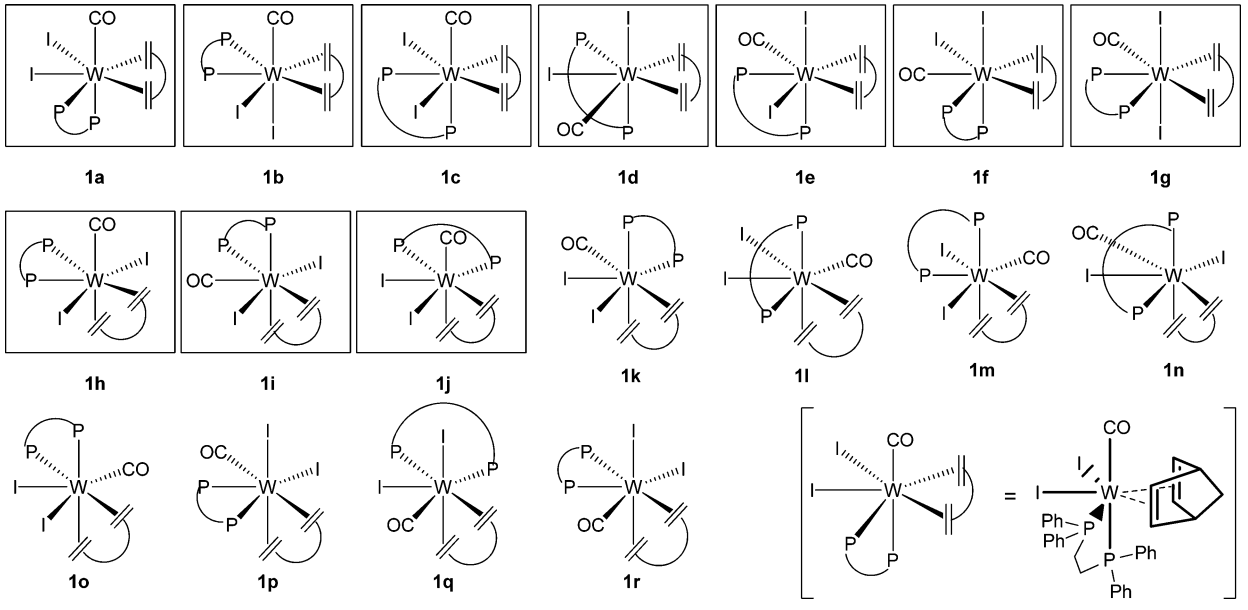

Figure 2. Eighteen hypothetical pentagonal bipyramidal configurational isomers. The boxed isomers are minima on the BP86 PES (see Table 3).

dx.doi.org/10.1021/om400667t | Organometallics 2013, 32, 5374–5383

Table 2. Effects of Ring Conformer and Phenyl Rotamer upon Stereoisomer Energy

configuration	ring conformer dihedral (deg) ϕ_r(PCCP)	phenyl rotamer dihedral (deg) ϕ_1(WPCC)	ϕ_2(WPCC)	ϕ_3(WPCC)	ϕ_4(WPCC)	labels[a]	E_{rel} (kcal mol^{-1})
1a	−59	152	80	28	98	GP,GP	0.0
1a	+49	147	77	168	88	GP,ZP	5.1
1a	+33	164	81	53	85	GP,EP	6.0
1b	−60	103	173	9	86	PZ,ZP	0.3
1b	−62	107	147	15	87	EG,GP	0.8
1b	−53	38	79	6	89	GP,ZP	1.8
1b	−41	21	80	77	157	GP,PG	3.3
1b	−56	68	49	75	77	EE,EP	6.8
1b	−51	107	130	66	18	EE,EG	6.8
1b	+48	53	78	24	87	EP,GP	0.4
1b	+45	60	38	23	87	EG,GP	0.9
1b	+51	46	82	62	77	EP,EP	2.1

[a]The letters are qualitative labels for these dihedrals: Z (cis) for ∼0 or ∼180°, G (gauche) for ∼30 or ∼150°, E (eclipsed) for ∼60 or ∼120°, P (panhandle) for ∼90°. The comma separates the phenyl dihedrals of one P (ϕ_1, ϕ_2) from phenyl dihedrals on the other P atom (ϕ_3, ϕ_4).

optimized BP86/basis2 energies from the single-point BP86/basis2//BP86/basis1 energies. Results from these corrections are reported only in Tables 9 and 10 in section 5.

3. RESULTS FOR THE W−DPPE COMPLEXES 1−5

3.1. Stereoisomers of 1. Given the restrictions that the bidentate ligands nbd and dppe must occupy two neighboring sites each, and the assumption of pentagonal-bipyramidal geometry, 18 different configurations are predicted (Figure 2). They were a posteriori labeled **1a−r** in order of increasing energy.

Preliminary optimizations of the 18 configurations identified **1a,b** as candidates for the most stable configurations. However, each configuration can feature the dppe ligand in a variety of possible phenyl group rotamers and two ring conformers (positive or negative twists) of the five-membered WPCCP ring. Hence, it is a difficult task to predict the lowest-energy stereoisomer of the entire complex.

We began by thoroughly exploring the phenyl rotamers and ring conformers of dppe within the **1a,b** configurations before choosing likely ones for all 18 configurational isomers for optimization. The resulting stereoisomers are given in Table 2. For **1a**, in which the dppe orientation is ax-eq (axial−equatorial), three unique stereoisomers were found with an energy span of 6.0 kcal mol^{-1}. For **1b**, in which the dppe orientation is eq-eq (equatorial−equatorial), nine unique stereoisomers were found with an energy span of 6.5 kcal mol^{-1}. The panhandle "P" position appears to be quite common for phenyl groups in dppe.

The number of stereoisomers is higher in the case of **1b**, in which dppe occupies an eq-eq orientation, than in **1a**, where dppe occupies an ax-eq orientation. The different number of stereoisomers seems to be due to the eq-eq-oriented nbd ligand, which imposes restrictions in the case of **1a**: nbd and two equatorial iodide ligands come nearer to the axial and equatorial phenyl rings of the dppe ligand, which restricts the second and fourth phenyl rings to have the "P" rotamer position (Figure 3). However, in **1b**, phenyl rings are farther away from nbd and iodide ligands, and therefore phenyl ring rotation and multiple rotamers are possible. Other than these observations, it seems quite difficult to predict which ring

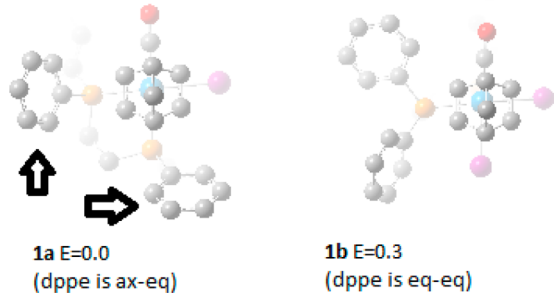

Figure 3. Depth-fog images of geometry-optimized examples of **1a,b** configuration isomers, showing in the **1a** case the two phenyl groups (see arrows) restricted to the panhandle rotamer position by virtue of their proximity to the nbd ligand. H atoms are deleted for clarity.

conformer and phenyl rotamers will be preferred for a given configurational isomer and ring conformer. What one can say is that rotamer variation affects the energy by up to 6.5 kcal mol^{-1}.

Next, stereoisomers of all 18 configurational isomers **1a−r** were pursued, and a total of 37 stereoisomers of $WI_2(CO)(\kappa^2P$-dppe$)(\eta^2{:}\eta^2$-nbd) (not including enantiomers) were located on the potential energy surface. Ten of the eighteen configurations (**1a−j**) were represented; no optimized stereoisomer structures could be found for configurations **1k−r**. Well over 80 optimizations were attempted, and there is no guarantee that this search has found all the stereoisomers that may exist on the DFT PES. Table 3 catalogs the results for the 37 structures, while Table 4 gives examples of unsuccessful runs.

From Table 3 one can see a large range of energies (41.5 kcal mol^{-1}) and some significant dependence of isomer energy upon ligand configuration. First, the $\eta^2{:}\eta^2$-nbd strongly prefers two cis-equatorial positions in this pentagonal-bipyramidal complex, since all configurations having an ax-eq nbd (**1h−r**) either do not exist as minima or lie >34 kcal mol^{-1} above the lowest-energy stereoisomer. Second, the most stable forms of **1a−g** are **1a−c**, because they have the σ-donor and π-acceptor carbonyl ligand in an axial position: if the carbonyl ligand is in the equatorial position, the E_{rel} values start at 8.7 kcal mol^{-1}. The least stable form of **1a−g** is **1g**, where the two iodide ligands

dx.doi.org/10.1021/om400667t | Organometallics 2013, 32, 5374−5383

Table 3. The 37 Unique (Energy-Distinct) Stereoisomers of 1 Found, BP86/basis1

config-uration	is nbd eq-eq?	is CO ax?	is dppe ax-eq?	dppe rotamer[a]	β_{PWP} (deg)	E_{rel} (kcal mol^{-1})
1a	Y	Y	Y	−GP,GP	81	0.0
1a	Y	Y	Y	+GP,ZP	81	5.1
1a	Y	Y	Y	+GP,EP	81	6.0
1b	Y	Y	N	−PZ,ZP	75	0.3
1b	Y	Y	N	+EP,GP	74	0.4
1b	Y	Y	N	−EG,GP	75	0.8
1b	Y	Y	N	+EG,GP	74	0.9
1b	Y	Y	N	−GP,ZP	75	1.8
1b	Y	Y	N	+EP,EP	74	2.1
1b	Y	Y	N	−GP,PG	76	3.3
1b	Y	Y	N	−EE,EP	75	6.8
1b	Y	Y	N	−EE,EG	76	6.8
1c	Y	Y	Y	−EE,EG	80	2.9
1c	Y	Y	Y	+GE,PG	80	3.2
1c	Y	Y	Y	−EE,GE	75	4.9
1d	Y	N	Y	+GP,GP	81	8.7
1d	Y	N	Y	−GE,GP	81	9.0
1d	Y	N	Y	+GP,EE	80	14.9
1e	Y	N	Y	−GE,PZ	78	8.8
1e	Y	N	Y	+ZE,PE	81	10.7
1e	Y	N	Y	+PE,PE	81	10.7
1e	Y	N	Y	−PG,GP	82	12.3
1e	Y	N	Y	−PG,EE	83	13.1
1e	Y	N	Y	−ZP,EP	80	15.0
1f	Y	N	Y	−GP,ZP	80	11.3
1f	Y	N	Y	+EE,GP	81	14.9
1g	Y	N	N	−PZ,EG	78	19.1
1g	Y	N	N	−PZ,PG	78	19.1
1g	Y	N	N	−PE,EP	79	19.5
1g	Y	N	N	+PZ,PE	78	19.5
1g	Y	N	N	−PE,PG	80	20.1
1h	N	Y	N	−ZP,ZP	75	34.3[b]
1h	N	Y	N	−EE,GE	78	37.4[b]
1h	N	Y	N	+PG,EE	78	38.4[b]
1i	N	N	Y	+PG,GP	83	35.3[b]
1j	N	Y	N	+EE,EZ	74	41.3[c]
1j	N	Y	N	+EE,EZ	74	41.5[c]

[a]Sign refers to sign of ϕ_r(PCCP). [b]During geometry optimization, η^2:η^2-nbd developed one strong η^2 and one weak η^2 interaction. [c]Distorted pentagonal bipyramid.

Table 4. Examples of Unsuccessful Runs

initial structure	is nbd eq-eq?	is CO ax?	is dppe ax-eq?	initial rotamer	result
1k	N	N	Y	PE,PP	**1d** (GP,GE)
1l	N	N	Y	GP,EE	**1a** (GP,GP)
1m	N	N	Y	GE,EE	EC[a]
1n	N	N	Y	PE,EE	**1d** (GP,GP)
1o	N	N	Y	PP,PE	EC[a]
1p	N	N	N	ZE,GP	**1a** (GP,GP)
1q	N	N	N	EP,EP	κ^1-dppe
1r	N	N	N	GG,EE	EC[a]

[a]Geometry optimization failed due to electronic convergence problem.

occupy the trans-axial positions of the pentagonal bipyramid. This order of preference for axial positions, $I^- < PR_3 < CO$, mimics the ordering of trans-directing power for similar reasons: PR_3 and particularly CO can obtain better overlap with donating d orbitals on W when in axial positions.

The global minimum of **1** at the BP86/basis1 level of theory is the −GP,GP stereoisomer of **1a**. There is, however, only a 0.25 kcal mol^{-1} energy difference between this and the −PZ,ZP stereoisomer of **1b,** a difference well within the expected accuracy of BP86/basis1. Reoptimization of the lowest-energy rotamer of **1a** and the seven lowest-energy rotamers of **1b** with BP86/basis2 resulted in an inverted preference for **1b**, a result we trust more but not completely. Hence, we cannot predict whether **1a** or **1b** will dominate the sample of **1**. It is surprising that both ax-eq and eq-eq positions are equally preferable for dppe ligands in this seven-coordinate tungsten complex. Even among the 10 possible configuration isomers **1a**−**j**, 6 of them have the dppe ligand in an ax-eq position. This ambiguity in orientation is suspected to be due to a balance between competing steric factors; one is bite angle strain and the other is phenyl repulsion strain. The natural bite angle[21] of dppe is 89°, calculated from $2\cdot\sin^{-1}(0.5R_{PP}/R_{WP})$, where R_{pp} comes from BP86 optimization on the free ligand (3.63 Å) and R_{wp} comes from the crystal structure[6] of $WI_2(CO)(\kappa^2P$-dppm$)(\eta^2$:η^2-nbd) (2.58 Å). The ideal angle between two ligands in a pentagonal bipyramid is 72° (eq-eq) or 90° (ax-eq), and hence bite angle strain is minimized in the ax-eq position. However, whenever dppe is in an ax-eq orientation of the pentagonal bipyramid, phenyl strain is large, because two phenyl rings on the equatorial phosphorus put pressure on all equatorial ligands. Hence, axial−equatorial and equatorial−equatorial orientations with different bite angles appear to generate equal amounts of total strain in the complex and therefore are predicted to be equally preferable for the dppe ligand in this complex.

To conclude this section, it must be emphasized that predicting the lowest-energy stereoisomer of a dppe-containing seven-coordinate complex is very hard work. However, in the absence of having an experimentally determined crystal structure, it is vitally important work for reaction energy prediction. Without a thorough search, one could obtain an energy for this complex (**1**) that is anywhere from 0 to 40 kcal/mol above its global minimum, causing up to 40 kcal/mol error in ΔE predictions.

3.2. Stereoisomers of 2−5. Computations of ligand binding energies of the seven-coordinate $WI_2(CO)(\kappa^2P$-dppe$)(\eta^2$:η^2-nbd) complex **1** require searches for the lowest-energy stereoisomers of the various six-coordinate fragmented complexes **2**−**5** that might result from detaching a metal−ligand bond. Conformer searching for **2**−**5** was performed by beginning with complexes **1a**,**b** (the two lowest-energy forms of **1**), removing a single coordination, and optimizing what was left. The lowest-energy structures were then rearranged and reoptimized for a greater sample set.

The configurational isomers obtained are summarized in Figure 4. Octahedral complexes were generally found for **2**−**5**, although for **4** and **5** some high-energy pentagonal-pyramidal structures were also found. An average of 3 stereoisomers per configurational isomer were optimized; in all, 9, 11, 9, and 17 stereoisomers were found for **2**−**5**, respectively, and details (including computed energies) are given in the Supporting Information.

For **2** (κ^2P-dppe → κ^1P-dppe), all four octahedral configuration isomers produced converged structures. The monodentate dppe ligand had dihedral angles of ϕ(WPCC) ≈ 60−90° and ϕ(PCCP) ≈ 180° in each case. The most stable stereoisomer of **2** had the **2a** configuration and the EP,ZE

dx.doi.org/10.1021/om400667t | Organometallics 2013, 32, 5374−5383

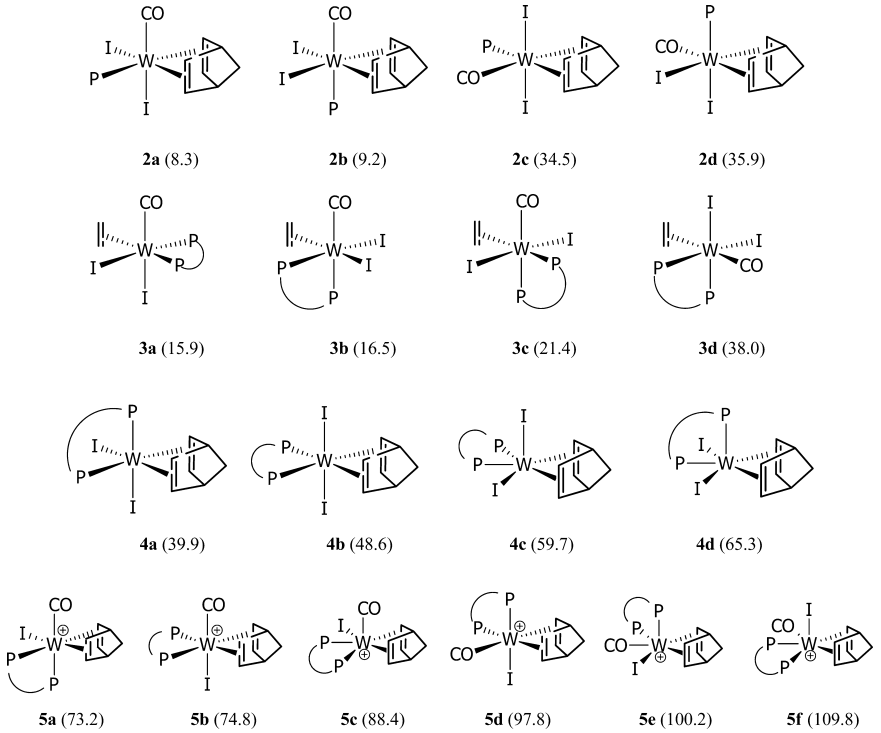

Figure 4. Configurational isomers found during geometry optimization of the fragmented six-coordinate complexes **2**–**5**. Numbers in parentheses are "appearance" energies ΔE (kcal mol^{-1}) for producing the lowest-energy stereoisomer of each configurational isomer, via ligand dissociation from the lowest-energy stereoisomer of **1**. The pentagonal-pyramidal structures are **4c,d** and **5c,e,f**.

rotamer combination for dppe, and its appearance energy (8.3 kcal mol^{-1}) is the W–P ligand binding energy in the parent seven-coordinate compound **1** at the BP86/basis1 "level of theory" (approximation for energy). While **2a,b** both have low-energy rotamers (ΔE = 8–9 kcal mol^{-1} in Figure 4), the **2c,d** configurations are substantially higher in energy (ΔE = 35–36 kcal mol^{-1}) due to the presence of a carbonyl ligand trans to an ene.

For **3** (η^2:η^2-nbd → η^2-nbd), four configurational isomers could be envisaged. In addition, the nbd could take regular or inverted positions (Figure 5). Regular positions were actually

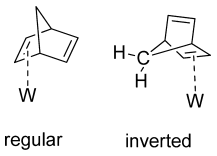

Figure 5. Positions of η^2-nbd observed in optimizations of **3**.

rare, for they were prone to full η^2:η^2 bonding (reverting to **1**); only one **3a** and one **3d** example were found. In the inverted position, the complex has an approximately seven-coordinate pentagonal-bipyramidal nature, with an optimized W–H distance of 2.5 Å to the nearest methylene H atom. In the lowest-energy form of **3a**, the H atom sits toward the equatorial iodide, and (assuming the W–H interaction to be negligible) its appearance energy of 15.9 kcal mol^{-1} is the W–ene binding energy at BP86/basis1 level of theory. As with **2**, the least favored configuration of **3** (**3d**) has the positioning of the carbonyl ligand trans to an ene.

For **4** (loss of CO), two octahedral configurations are possible, with the cis-I version (40–44 kcal mol^{-1}) lower than the trans-I version (49–56 kcal mol^{-1}). Two higher-energy pentagonal pyramid structures were also found (**4c,d**, 60–65 kcal mol^{-1}). Pentagonal-pyramidal structures have been observed for some W^{VI} anion complexes in solution.[22]

For **5** (loss of I$^-$), all three octahedral and three pentagonal-pyramidal structures were observed. Of the octahedral configurations, **5a,b** are significantly more stable than **5d** because they avoid a CO–W–ene *trans* geometry. Of the pentagonal-pyramidal configurations, **5c** is more stable than **5e,f** for the same reasons, although CO is not perfectly trans to an ene in **5e** or **5f**.

3.3. Appearance Energies of 2–5. Figure 6 is a summary plot of the range of appearance energies calculated from the lowest-energy stereoisomer of **1** to the various stereoisomers of **2**–**5**, respectively. The "ligand binding energy" (gas phase, uncorrected for zero-point or thermal effects and approximated by the BP86/basis1 level of theory) would be the lowest

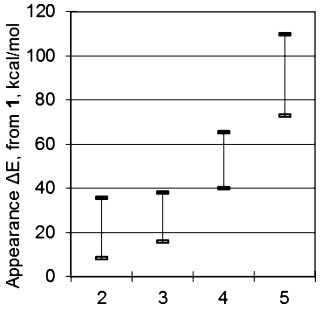

Figure 6. Ranges of computed appearance energies for various stereoisomers of **2** (W–P dissociation), **3** (W–ene), **4** (W–CO), and **5** (W–I$^-$) from the parent dppe-containing compound **1**. The ligand binding energy (at this level of approximation) would be the lowest value in each range.

dx.doi.org/10.1021/om400667t | *Organometallics* 2013, 32, 5374–5383

appearance energy, i.e., the lower limit of these ranges. We postpone a discussion of the ligand binding energies to the end of the paper, but here with the large ranges in Figure 6 we hope to convince the reader that the computation of such binding energies depends *crucially* on finding lowest-energy stereoisomers of the parent and of the dissociated fragment.

4. RESULTS FOR THE W–DPPM COMPLEXES 6–10

4.1. Stereoisomers of 6. Turning now to the W–dppm parent complex **6**, we searched the same set of 18 hypothetical configuration isomers **a**–**r** as in the case of the W–dppe complex **1**. Only 9 of the 18 configurations are minima for **6** on the BP86 potential energy surface. This is 1 less than for **1**, the only difference being that the **1i** configuration has no **6i** counterpart.

Similar to the case for the tungsten–dppe complex, each of the 18 configurational isomers of the tungsten–dppm complex can also feature the dppm ligand in a variety of possible phenyl group rotamers. Unlike the W–dppe case, in W–dppm there are no positive and negative ring conformer options with the WPCP four-membered ring; only one option existed per phenyl rotamer set. Starting as we did with **1**, we first searched for many phenyl rotamers of the **6a** and **6b** configurational isomers, and again, as with **1a**,**b**, many more stereoisomers of the **b** configuration were found, spanning a similar 6 kcal mol^{-1} energy range (Table 5).

Table 5. Effects of Phenyl Rotamer upon Stereoisomer Energy for 6b

phenyl rotamer dihedrals (deg)					
ϕ_1 (WPCC)	ϕ_2 (WPCC)	ϕ_3 (WPCC)	ϕ_4 (WPCC)	labels[a]	E_{rel} (kcal mol^{-1})
52	84	169	83	EP,ZP	0.0
70	11	174	84	EZ,ZP	0.3
37	82	79	165	GP,PZ	0.4
94	164	1	85	PG,ZP	0.9
46	88	155	108	EP,GE	1.1
139	37	93	20	GG,PG	2.6
34	83	73	68	GP,EE	3.9
103	144	86	2	PG,PZ	4.8
135	24	100	105	EG,PE	6.0
48	153	70	72	EG,EE	6.0
136	29	100	100	GG,PP	6.1

[a]The letters are qualitative labels for these dihedrals: Z (cis) for ~0 or ~180°, G (gauche) for ~30 or ~150°, E (eclipsed) for ~60 or ~120°, P (panhandle) for ~90°. The comma separates the phenyl dihedrals of one P (ϕ_1, ϕ_2) from phenyl dihedrals on the other P atom (ϕ_3, ϕ_4).

Next, stereoisomers of all 18 configurational isomers **6a**–**r** were pursued, and out of over 75 attempts, a total of 31 stereoisomers of $WI_2(CO)(\kappa^2P$-dppm$)(\eta^2{:}\eta^2$-nbd) (not including enantiomers) were located on the potential energy surface. Nine of the 18 configurations (**1a**–**h**,**j**) were represented. Table 6 catalogs the results for the 31 structures, while Table 7 gives examples of unsuccessful runs.

As in **1**, in **6** there is strong preference for nbd to be eq-eq, since all configurations in which nbd is ax-eq (**6h**–**r**) either do not exist or lie >24 kcal mol^{-1} above the lowest-energy stereoisomer. Given an eq-eq nbd (**6a**–**g**), the most stable forms are **6a**–**c**, which have an axial CO ligand, and the least stable form is **6g**, in which two iodide ligands occupy the trans-

Table 6. The 31 Unique (Energy-Distinct) Stereoisomers of 6 Found, BP86/basis1

configuration	is nbd eq-eq?	is CO ax?	is dppm ax-eq?	dppm rotamer	β_{PWP} (deg)	E_{rel} (kcal mol^{-1})
6a	Y	Y	Y	GP,GP	68	7.7
6b	Y	Y	N	EP,ZP	64	0.0
6b	Y	Y	N	EZ,ZP	64	0.3
6b	Y	Y	N	GP,PZ	65	0.4
6b	Y	Y	N	PG,ZP	65	0.9
6b	Y	Y	N	EP,GE	63	1.1
6b	Y	Y	N	GG,PG	65	2.6
6b	Y	Y	N	GP,EE	66	3.9
6b	Y	Y	N	PG,PZ	66	4.8
6b	Y	Y	N	EG,PE	66	6.0
6b	Y	Y	N	EG,EE	66	6.0
6b	Y	Y	N	GG,PP	66	6.1
6c	Y	Y	Y	PG,GP	65	8.4
6c	Y	Y	Y	EG,GE	66	10.3
6c	Y	Y	Y	EE,PG	67	11.1
6d	Y	N	Y	GP,GP	68	12.6
6d	Y	N	Y	GE,PE	68	19.3
6e	Y	N	Y	GE,PZ	66	13.0
6e	Y	N	Y	GP,PG	67	14.7
6e	Y	N	Y	EE,GP	68	15.6
6e	Y	N	Y	GE,EP	68	16.8
6e	Y	N	Y	GE,GP	68	16.8
6e	Y	N	Y	EE,GP	67	16.9
6f	Y	N	Y	EE,ZP	68	18.0
6f	Y	N	Y	GE,GP	68	18.0
6g	Y	N	N	GP,PG	65	21.2
6g	Y	N	N	PG,GP	65	21.2
6g	Y	N	N	EP,GE	66	24.4
6h	N	Y	N	GP,ZE	65	28.2[a]
6h	N	Y	N	ZE,GE	66	31.4
6j	N	Y	N	ZG,PG	63	42.0[b]

[a]During geometry optimization, $\eta^2{:}\eta^2$-nbd developed one strong η^2 and one weak η^2 interaction. [b]Distorted pentagonal bipyramid.

Table 7. Examples of Unsuccessful Runs

initial structure	is nbd eq-eq?	is CO ax?	is dppm ax-eq?	initial rotamer	result
6i	N	N	Y	PG,GP	**6b** (EZ,ZP)
6k	N	N	Y	EP,PP	BD[a]
6l	N	N	Y	EP,EP	BD[a]
6m	N	N	Y	EP,PE	BD[a]
6n	N	N	Y	PE,EP	**6g** (EZ,GP)
6o	N	N	Y	EE,PP	EC[b]
6p	N	N	N	PG,PP	**6e** (GE,GP)
6q	N	N	N	PG,EE	**6c** (GP,PG)
6r	N	N	N	GE,PP	EC[b]

[a]Bond dissociation within dppm: P–CH_2 rupture. [b]Electronic convergence failure.

axial position of the pentagonal bipyramid; again, all this is similar to the W–dppe case **1**.

The global minimum of **6** at the BP86/basis1 level of theory is the EP,ZP stereoisomer of the **6b** configuration. The lowest-energy stereoisomer of the next stable configuration, **6a** (GP,GP), is higher in energy by 7.7 kcal mol^{-1}, a large enough gap to allow the conclusion that configuration **6b** is expected to dominate in a sample of **6**. This is different than the case of the

dx.doi.org/10.1021/om400667t | *Organometallics* 2013, 32, 5374–5383

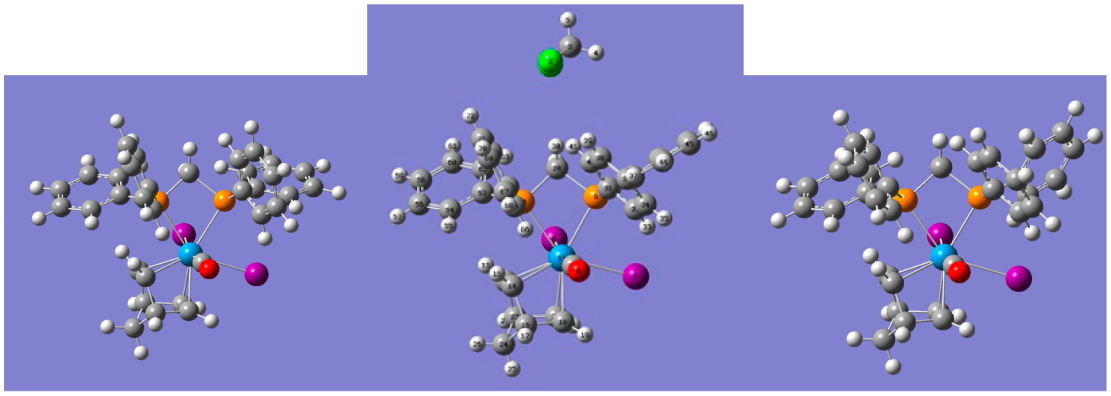

Figure 7. Comparison of the lowest-energy predicted stereoisomers of **6** (BP86/basis1) with that found experimentally in the crystal of **6**:CH_2Cl_2. The only significant discrepancy is in the ϕ_2(WPCC) phenyl rotamer dihedral angle of the phenyl group in the back upper right of each image; the experimental value (49°) is an average of the values seen in our two lowest-energy predictions (84° in EP,ZP and 11° in EZ,ZP) and could be due to a crystal-packing effect.

tungsten−dppe complex, where the calculated BP86/basis1 energy difference between **1a** and **1b** is only 0.25 kcal/mol. The clear preference for the eq-eq orientation of dppm is because both bite angle strain and phenyl strain are minimized in this orientation. The natural bite angle[21] of dppm is 73°, as calculated from $2{\cdot}\sin^{-1}(0.5R_{PP}/R_{WP})$, where R_{pp} comes from BP86 optimization on the free ligand (3.07 Å) and R_{wp} comes from the crystal structure[6] of $WI_2(CO)$(dppm-κ^2P)(η^2:η^2-nbd) (2.58 Å). Since the ideal angle between two ligands in a pentagonal bipyramid is 72° (eq-eq) or 90° (ax-eq), the bite angle strain is minimized by the eq-eq orientation (unlike the dppe case). The phenyl strain is also minimized by the eq-eq orientation (like the dppe case).

We can compare to the structure of **6** found in the 1:1 crystal **6**:CH_2Cl_2 (Supporting Information), a compound isolated in our laboratories a few years ago.[6] The stereoisomer in the crystal is **6b** (EE,ZP), which is *nearly identical* with our lowest two predictions (Figure 7), supporting our methodology. Table 8 gives a quantitative comparison of selected parameters.

Table 8. Comparison of Selected Internal Coordinates of 6

coordinate	exptl value **6**:CH_2Cl_2	BP86/basis1 **6b** (EZ,ZP)
R(W−P_1) (Å)	2.593(1)	2.609
R(W−P_2) (Å)	2.570(1)	2.596
R(W−I_1) (Å)	2.9009(4)	2.927
R(W−I_2) (Å)	2.8623(4)	2.911
R(W−CO) (Å)	1.937(5)	1.938
θ(PCP) (deg)	95.9(2)	95.8
θ(PWP) (deg)	63.71(4)	64.2
ϕ_1(WPCC) (deg)	70.5(5)	70
ϕ_2(WPCC) (deg)	48.6(6)	11
ϕ_3(WPCC) (deg)	170.0(3)	174
ϕ_4(WPCC) (deg)	81.1(5)	84

It is concluded that the prediction of the lowest-energy stereoisomer of the dppm-containing seven-coordinate complex **6** has an additional rule of thumb in comparison to the dppe-containing complex **1**: as well as having nbd eq-eq and CO axial, dppm should be eq-eq. This restricts the lowest-energy stereoisomer to configuration **6b**. The phenyl rotamers are still difficult to predict, however, but a thorough search of the rotamers succeeded in essentially matching the stereoisomer observed in the crystal.

4.2. Stereoisomers of 7−10. The same conformer search strategy was used as for **2**−**5**, resulting in 5, 12, 5, and 8 stereoisomers of **7**−**10**, respectively. The same configurational isomers as in Figure 4 for **2**−**5** were observed from optimizations of **7**−**10**, and hence the **a**−**f** configuration designations are kept identical for ease of comparison.

For **7** (κ^2P-dppm → κ^1P-dppm), the structures and trends (but not the phenyl rotamers) are similar to those of **2**, as might be expected for monodentate κ^1P versions of dppm and dppe. For **8** (η^2:η^2 → η^2-nbd), **9** (CO dissociation), and **10** (I^- dissociation), the trends are also similar to their dppe-containing counterparts (**3**−**5**, respectively).

4.3. Appearance Energies of 7−10. Figure 8 is a summary plot of the range of appearance energies calculated

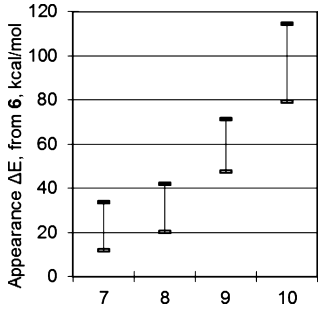

Figure 8. Ranges of computed appearance energies for various stereoisomers of **7** (W−P dissociation), **8** (W−ene), **9** (W−CO), and **10** (W−I^-) from the parent dppm-containing compound **6**. The ligand binding energy (at this level of approximation) would be the lowest value in each range.

from the lowest-energy stereoisomer of **6** to the various stereoisomers of **7**−**10**, respectively. These ranges are very similar to those in Figure 6. The most important difference is that the ligand binding energies, the lower limits of each range, are 4−8 kcal mol^{-1} higher than in Figure 6, *for every ligand in the complex*; this is discussed further in the next section.

4.4. Ligand Binding Energies of 1 and 6. Using the lowest appearance energies for **2**−**5** and **7**−**10** (Supporting

dx.doi.org/10.1021/om400667t | *Organometallics* 2013, 32, 5374−5383

Table 9. Alternative Energy Corrections δE_{rel} (kcal mol^{-1}) for the Low-Energy Stereoisomers of Compounds 1−10

stereoisomer	E_{rel}	δE_{rel}(ZPVE)	δE_{rel}(basis2)	δE_{rel}(relax)	δE_{rel}(toluene)	δE_{rel}(dispersion)
1a	**0.0**					
1b, rotamer 1	**0.2**	0.1	−6.9	1.4	0.6	1.6
1b, rotamer 2	**0.3**	0.2	−5.1	1.8	0.3	0.9
1b, rotamer 3	**0.7**	−0.1	−5.5	dne[a]	0.4	2.0
1b, rotamer 4	**0.9**	0.0	−5.6	dne[a]	0.6	1.6
1b, rotamer 5	**1.7**	−0.5	−7.2	1.2	0.6	2.1
1b, rotamer 6	**2.1**	0.2	−5.3	dne[a]	0.1	−0.8
1b, rotamer 7	**3.3**	0.0	−5.1	1.8	0.4	1.3
2a	**8.3**	−2.1	1.3	−1.8	0.6	9.5
2b	**9.1**	−0.9	−5.1	−5.0	3.2	8.1
3a	**15.9**	−0.6	−6.8	1.4	0.2	3.0
3b	**16.5**	−0.8	−3.1	0.2	0.9	0.7
4a + CO	**39.9**	−3.6	−4.6	−0.1	0.1	3.9
5a + I$^-$	**73.1**	−2.0	21.2	−2.8	−49.4	3.9
6a	**0.0**					
6b, rotamer 1	**-7.7**	0.1	−4.9	2.0	0.7	0.1
6b, rotamer 2	**-7.4**	−0.1	−5.7	2.2	1.0	0.0
6b, rotamer 3	**-7.3**	0.2	−4.9	2.3	0.6	−0.7
6b, rotamer 4	**-6.8**	0.1	−5.8	dne[a]	0.9	0.3
6b, rotamer 5	**-6.6**	−0.1	−6.7	dne[a]	0.8	−0.6
6b, rotamer 6	**-5.1**	0.6	−5.2	2.5	0.8	0.5
6b, rotamer 7	**-3.8**	0.4	−4.5	dne[a]	0.2	−1.7
7a	**4.3**	−1.1	4.5	−2.9	1.0	1.9
7b	**5.8**	−0.1	−6.2	−1.2	3.7	6.0
8a	**12.7**	−0.5	−8.2	1.8	0.4	2.6
8b	**16.0**	−0.7	−2.6	0.4	1.1	2.4
9a + CO	**39.9**	−2.9	−4.0	0.5	0.5	4.7
10a + I$^-$	**71.4**	−1.4	21.8	−0.7	−49.1	3.6

[a]dne: does not exist (reoptimization led to a different rotamer).

Information), the BP86/basis1 uncorrected gas-phase ligand binding energies for {W−P, W−ene, W−CO, and W−I$^-$} are {12, 20, 48, 79} kcal mol^{-1} for the W−dppm complex **6** and {8, 16, 40, 73} for the W−dppe complex **1**. The binding energies for {M−P, M−ene, and M−CO} in the less-strained $L_2Mo(CO)_4$ complexes of Mukerjee et al. are {35−43, 27, 35−41} kcal mol^{-1},[23] and thus one sees the significant weakening of the M−P bond strengths in these seven-coordinate W complexes (despite the ability of diphosphines to "twist" or "tilt" their P lone pairs to maintain bond strength in mildly strained situations[24]).

Thus, at the level of theory, it appears that the larger bite angle of dppe in **1** (versus dppm in **6**) reduces *all* ligand binding energies. For alternative estimates of these ligand binding energies, we considered five possible "improvements" to the energy approximation, although improved accuracy with any of these corrections cannot be guaranteed.

Several low-lying isomers of each compound **1**−**10** had their energies recomputed five times to test five energy corrections: (i) zero-point vibrational energies (ZPVE), (ii) continuum solvation effect (solvent=toluene), (iii) intramolecular attractive London dispersion energy, (iv) basis-set improvement effects (to basis2: replacing all STO-3G atoms with 6-31G(d) atoms), and (v) geometry reoptimization ("relaxation") effects with the basis set basis2. Total energies appear in the Supporting Information. Table 9 contains BP86/basis1 relative energies for each stereoisomer (E_{rel}) plus the five computed correction terms for consideration.

First, the ZPVE corrections (column 3 in Table 9) are all below 1 kcal mol^{-1} except for **2a**/**5a**/**7a**/**10a** (−1.1 to −2.1) and **4a**/**9a** (−2.9 to −3.6), which have reduced structural rigidity. Second, the improved basis set revealed an increased amount of repulsion between the nbd ligand and any neighboring phenyl ring (which optimized too closely to nbd due to its restrictive STO-3G basis set); this extra repulsion shifts up the energies of **1a** and **6a** by 6 kcal mol^{-1}, resulting in the general shift of −6 kcal mol^{-1} of most other compounds relative to them (column 4). However, for iodide dissociation, this basis1 → basis2 energy correction is very large (+21 to +22 kcal mol^{-1}) because differential STO-3G errors appear in going from neutral parent (**1** and **6**) to cation (**5** and **10**); the replacement of STO-3G likely benefits the electronic distributions of neutral species more substantially than those of cations. Third, relaxation effects (column 5) generally dampen the aforementioned repulsion effect by 20−40% except in rare instances. These three corrections are likely to improve the calculation.

The fourth correction, for toluene solvation, is generally less than 1 kcal mol^{-1}, but the overly large prediction of a −49 kcal mol^{-1} effect for iodide dissociation makes the continuum solvation model look poor. The fifth correction, for dispersion attraction, varies up to 3 kcal mol^{-1} except for dissociations of CO and iodide (+3.6 to +4.7 kcal mol^{-1}) and the W−P dissociations (1.9 to 9.5 kcal mol^{-1}). These larger dispersion corrections may be appropriate for the gas phase, where the CO, iodide, or two phenyl groups are leaving the attractive region of the complex, but this would not be appropriate for a solution in toluene, where toluene molecules can offer compensatory dispersion attraction. Hence, we think the

dx.doi.org/10.1021/om400667t | *Organometallics* 2013, 32, 5374−5383

continuum solvation and dispersion corrections do more harm than good in this work.

Hence, for "improved" ligand binding energies, the sums $E_{rel,new} = E_{rel,old} + \delta E_{rel}(ZPVE) + \delta E_{rel}(basis2) + \delta E_{rel}(relax)$ were made, the results rezeroed to **1b** (rotamer 1) and **6b** (rotamer 2) to become appearance energies, and the lowest appearance energies for **2**−**5** and **7**−**10** became the improved ligand binding energies for {W−P, W−ene, W−CO, and W−I$^-$}: they are {9, 17, 44, 102} kcal mol^{-1} for the W−dppm complex **6** and {3, 15, 37, 95} kcal mol^{-1} for the W−dppe complex **1**. Thus, all four ligand binding energies are still predicted to fall with increasing bite angle (dppm → dppe, **6** → **1**), and the reductions (ΔD_e, Table 10) are each within 2 kcal mol^{-1} of the original BP86/basis1 shifts, but now the bite angle effect reduces the W−ene D_e noticeably less than the others.

Table 10. Shifts (Δ) in Selected Bond Properties Upon Replacing dppm by dppe in 1[a]

W−X	ΔD_e(WX), **6** → **1**	ΔR_i(WX), **6** → **1**	$\Delta(R_f[WP] - R_i[WP])$, **6** → **1**
W−P[b]	−6	0.07	−0.08
W−ene[c]	−2	0.01	0.00
W−CO[d]	−7	0.00	−0.05
W−(I$^-$)[d]	−7	0.00	−0.10

[a] D_e data from basis2 + ZPVE(basis1); bond length data from BP86/basis2 reoptimization. [b] The P closest to the equatorial I in the **b** configurations of **1** and **6**; see Figure 2. [c] R(W−ene) is taken to be the average of the four R(W−C) values. [d] Axial ligand.

Having faith in the improved values, we wanted to understand why the bite angle increase would affect the W−ene binding energy less than the other ligand binding energies. Table 10 gives these binding energy shifts together with bond length information. Often a dissociation energy (column 2) is correlated with the bond length before dissociation (column 3); a "weakened" bond is expected to have a positive ΔR somewhat proportional to its negative ΔD_e. However, in Table 10 this correlation fails, since *the bite angle increase did not appreciably alter the metal−ligand bond lengths* except in the bidentate ligand itself. How, then, is the dppe ligand managing to reduce the dissociation energies of its axial CO and iodide ligands without altering their metal−ligand bond lengths?

We propose the following resolution. One can keep the comforting inverse relationship of bond "strength" to bond length but then recognize that a dissociation energy in a polyatomic molecule (and hence a ligand binding energy in an organometallic complex) is this bond "strength" *minus* a relaxation energy of the ensuing dissociated pieces. Seen in this way, the 7 kcal mol^{-1} reduction (due to increased bite angle) of the dissociation energies of the axial CO and iodide ligands is not due to a reduction in bond "strength" (since their bond lengths did not change) but due to an increase in relaxation energy when dissociating from **1** versus **6**. This increase in relaxation energy is directly due to the larger bite angle, which causes more initial strain in the seven-coordinate parent (**1** versus **6**) and thus more energy liberation during any ligand dissociation. The larger strain in **1** does not affect each W−X bond length equally, but due to product relaxation it should affect each W−X binding energy equally. A reasonable measure of the strain and general relaxation in **1** and **6** is the larger of the two W−P bond lengths, which exhibits the extra strain inherent in **1** versus **6** (2.69 versus 2.62 Å), yet generally equal amounts of strain in the comparable six-coordinate products (i.e., after W−CO dissociation, 2.57 versus 2.58 Å in **4** versus **9**). The fourth column in Table 10, which uses this metric, shows a crude correlation with the bite angle effects on the binding energies.

The reason that the W−ene D_e is not affected as much as the others by the increase in bite angle is because the product after dissociation of one ene (**3** or **8**) is not truly six-coordinate, due to inversion of the nbd unit (recall Figure 5), and this greatly dampens the relaxation effect. Hence, for seven-coordinate tungsten complexes, we conclude that an increase in bite angle of a bidentate ligand will generally make all ligands more labile due to the rise in strain energy of the seven-coordinate species, and the common release of this strain during all normal (i.e., coordination-reducing) ligand dissociations.

5. CONCLUSIONS

The computation of ligand binding energies requires the determination of lowest-energy stereoisomers, and this is challenging. For **1** and **6**, 18 different configurational isomers are possible; half of these exist as local minima on the BP86 potential energy surface, and they span ∼42 kcal mol^{-1} in energy. In total, 37 energy-distinct stereoisomers of **1** and 31 of **6** were found on the PES, due not only to variance in configuration but also to the presence of dppe or dppm, which contain multiple internal rotation coordinates with energy effects of up to 7 kcal mol^{-1}.

Generally, the preferred configurations of the pentagonal-bipyramidal complexes **1** and **6** have η^2:η^2-nbd in an eq-eq orientation, κ^2*P*-dppm in an eq-eq orientation, and a carbonyl ligand in an axial position. Hence, the preferred configuration for the $WI_2(CO)(\kappa^2P\text{-dppm})(\eta^2{:}\eta^2\text{-nbd})$ complex **6** is uniquely **6b**, a prediction confirmed by our experimental crystal structure of the 1:1 crystal **6**:CH_2Cl_2. The κ^2*P*-dppe ligand, with its natural bite angle of 89°, does not automatically take the expected ax-eq orientation because this produces counter-balancing equatorial strain due to phenyl group positioning, and hence for the $WI_2(CO)(\kappa^2P\text{-dppe})(\eta^2{:}\eta^2\text{-nbd})$ complex **1**, the BP86/basis2 prediction (which actually favors eq-eq **1b** over ax-eq **1a**) is not as definitive.

Ligand binding strengths in **1** and **6** increase in the order W−P < W−ene < W−CO < W$^+$−I$^-$, an ordering predicted to exist in the gas phase and in nonaqueous solutions (aqueous solutions would likely stabilize the W$^+$−I$^-$ dissociation and react with the ensuing cationic complex). Although the W−P and W−ene bonds are the weakest (3−9 and 15−17 kcal mol^{-1}, respectively), the chelation effect may make them less important than W−CO dissociation (37−44 kcal mol^{-1}) in terms of activity. Regardless of which dissociation is relevant, switching from the known dppm compound **6** to the unknown dppe compound **1** reduces *every* binding energy in the complex by 2−7 kcal mol^{-1}. Since the case of W−ene dissociation is rather odd here (resulting in an essentially seven-coordinate product), the typical reduction in W−X D_e is predicted to be 6−7 kcal mol^{-1}. Thus, the increased actual bite angle of dppe vs dppm (74 vs 64°) puts an extra steric strain of 6−7 kcal mol^{-1} on the parent complex, principally among the equatorial ligands (as the axial bond lengths are not affected; Table 10), and this extra strain results in larger product relaxation energies and hence lowered dissociation energies for all coordination-reducing ligand dissociations.

dx.doi.org/10.1021/om400667t | *Organometallics* 2013, 32, 5374−5383

Finally, assuming the steric rule for reactivity as stated in the Introduction, switching from dppm to dppe is predicted to increase activity if the rate-limiting step is ligand loss but decrease activity if the rate-limiting step is the coordination of a new substituent.

■ ASSOCIATED CONTENT

Supporting Information

Tables of stereoisomers of **2**−**5** and **7**−**10**, total energies for Table 9, and Cartesian coordinates of all stereoisomers of **1**−**10** and a CIF file giving crystallographic data for **6**:CH_2Cl_2. This material is available free of charge via the Internet at http://pubs.acs.org.

■ AUTHOR INFORMATION

Corresponding Author

*E-mail for A.L.L.E.: allan.east@uregina.ca.

Notes

The authors declare no competing financial interest.

■ ACKNOWLEDGMENTS

We thank the Natural Science and Engineering Research Council and the Canada Foundation for Innovation for funding and the Laboratory for Computational Discovery (Regina) for supercomputer maintenance.

■ REFERENCES

(1) Kranenburg, M.; van der Burgt, Y. E. M.; Kamer, P. C. J.; van Leeuwen, P. W. N. M. *Organometallics* **1995**, *14*, 3081.
(2) (a) van der Veen, L. A.; Keeven, P. H.; Schoemaker, G. C.; Reek, J. N. H.; Kamer, P. C. J.; van Leeuwen, P. W. N. M.; Lutz, M.; Spek, A. L *Organometallics* **2000**, *19*, 872. (b) Bronger, R. P. J.; Kamer, P. C. J.; van Leeuwen, P. W. N. M. *Organometallics* **2003**, *22*, 5358.
(3) Although van Leeuwen and co-workers had speculated about an electronic bite angle effect for hydroformylation,[4a] their later work[4b] acknowledges steric effects as well.
(4) (a) Freixa, Z.; van Leeuwen, P. W. N. M. *Dalton Trans.* **2003**, 1890. (b) Zuidema, E.; Goudriaan, P. E.; Swennenhuis, B. H. G.; Kamer, P. C. J.; van Leeuwen, P. W. N. M.; Lutz, M.; Spek, A. L. *Organometallics* **2010**, *29*, 1210.
(5) (a) van Zeist, W.-J.; Visser, R.; Bickelhaupt, F. M. *Chem. Eur. J.* **2009**, *15*, 6112. (b) van Zeist, W.-J.; Bickelhaupt, F. M. *Dalton Trans.* **2011**, *40*, 3028.
(6) Tosh, E. K. M.Sc.Thesis, University of Regina, Regina, Canada, 2006.
(7) Amas, A. J.; McGourtery, T. A.; Tuck, C. N. *Eur. Polym. J.* **1976**, *12*, 93.
(8) Sen, A.; Thomas, R. R. *Organometallics* **1982**, *1*, 1251.
(9) (a) Szymańska-Buzar, T.; Glowiak, T.; Czeluśniak, I. *J. Organomet. Chem.* **2001**, *640*, 72. (b) Szymańska-Buzar, T.; Glowiak, T.; Czeluśniak, I. *Polyhedron* **2002**, *21*, 2505.
(10) Baker, P. K.; Drew, M. G. B.; Meehan, M. M.; Müller, J. *Z. Anorg. Allg. Chem.* **2002**, *628*, 1727.
(11) Bencze, L.; Bíró, N.; Szabó-Ravasz, B.; Mihichuk, L. *Can. J. Chem.* **2004**, *82*, 499.
(12) Handzlik, J.; Górski, M.; Szymańska-Buzar, T. *J. Mol. Struct. (THEOCHEM)* **2005**, *718*, 191.
(13) Handzlik, J.; Stosur, M.; Kochel, A.; Szymańska-Buzar, T. *Inorg. Chim. Acta* **2008**, *502*, 41.
(14) East, A. L. L.; Berner, G. M.; Morcom, A. D.; Mihichuk, L. *J. Chem. Theory Comput.* **2008**, *4*, 1274.
(15) Jayaraman, A.; Berner, G. M.; Mihichuk, L. M.; East, A. L. L. *J. Mol. Catal. A: Chem.* **2011**, *351*, 143.
(16) Frisch, M. J.; Trucks, G. W.; Schlegel, H. B.; Scuseria, G. E.; Robb, M. A.; Cheeseman, J. R.; Scalmani, G.; Barone, V.; Mennucci, B.; Petersson, G. A.; Nakatsuji, H.; Caricato, M.; Li, X.; Hratchian, H. P.; Izmaylov, A. F.; Bloino, J.; Zheng, G.; Sonnenberg, J. L.; Hada, M.; Ehara, M.; Toyota, K.; Fukuda, R.; Hasegawa, J.; Ishida, M.; Nakajima, T.; Honda, Y.; Kitao, O.; Nakai, H.; Vreven, T.; Montgomery, J. A., Jr.; Peralta, J. E.; Ogliaro, F.; Bearpark, M.; Heyd, J. J.; Brothers, E.; Kudin, K. N.; Staroverov, V. N.; Kobayashi, R.; Normand, J.; Raghavachari, K.; Rendell, A.; Burant, J. C.; Iyengar, S. S.; Tomasi, J.; Cossi, M.; Rega, N.; Millam, J. M.; Klene, M.; Knox, J. E.; Cross, J. B.; Bakken, V.; Adamo, C.; Jaramillo, J.; Gomperts, R.; Stratmann, R. E.; Yazyev, O.; Austin, A. J.; Cammi, R.; Pomelli, C.; Ochterski, J. W.; Martin, R. L.; Morokuma, K.; Zakrzewski, V. G.; Voth, G. A.; Salvador, P.; Dannenberg, J. J.; Dapprich, S.; Daniels, A. D.; Farkas, Ö.; Foresman, J. B.; Ortiz, J. V.; Cioslowski, J.; Fox, D. J. *Gaussian 09, Revision C.01*; Gaussian, Inc., Wallingford, CT, 2009.
(17) Wadt, W. R.; Hay, P. J. *J. Chem. Phys.* **1985**, *82*, 284.
(18) Hay, P. J.; Wadt, W. R. *J. Chem. Phys.* **1985**, *82*, 299.
(19) Scalmani, G.; Frisch, M. J. *J. Chem. Phys.* **2010**, *132*, 114110.
(20) Grimme, S. *J. Comput. Chem.* **2006**, *27*, 1787.
(21) Van Leeuwen, P. W. N. M.; Kamer, P. C. J.; Reek, J. N. H. *Pure Appl. Chem.* **1999**, *71*, 1443.
(22) Piquemal, J.-Y.; Halut, S.; Bregeault, J.-M. *Angew. Chem., Int. Ed.* **1998**, *37*, 1146.
(23) Mukerjee, S. L.; Nolan, S. P.; Hoff, C. D.; Lopez de la Vega, R. *Inorg. Chem.* **1988**, *27*, 81.
(24) Lichtenberger, D. L.; Jatcko, M. E. *J. Coord. Chem.* **1994**, *32*, 79.